Pergamon

Journal of Structural Geology, Vol. 17, No. 3, pp. 451 to 454, 1995

0191-8141/95 $9.50 + 0.00

0191-8141(94)00096-4

Stress and strain estimates for Newtonian and non-Newtonian materials in a rotational shear zone

TOSHIAKI MASUDA, NAOYA MIZUNO, MADOKA KOBAYASHI and TRAN NGOC NAM

Institute of Geosciences, Shizuoka University, Shizuoka 422, Japan

and

SHIGERU OTOH

Department of Earth Sciences, Toyama University, Toyama 930, Japan

(*Received* 21 *February* 1994; *accepted in revised form* 31 *August* 1994)

Abstract—Stress and shear strain rate in a rotational shear zone between two concentric circular boundaries are estimated for both Newtonian and non-Newtonian materials. Tangential shear stress in the shear zone $\tau_{r\theta}$ is proportional to $1/r^2$, where r is distance from the centre of rotation. The principal stresses σ_1 and σ_3 at a point are oriented at 45° to the radius through the point from the centre of rotation. The shear strain rate $\dot{\gamma}$ is proportional to $1/r^{2n}$, where n is the stress exponent in the constitutive equation. The distribution of strain ellipses systematically varies from place to place as a function of the total angle of rotation of the circular boundaries and of n. Deformation appears prominently concentrated in a narrow zone close to the interior boundary when n becomes large.

INTRODUCTION

A rotational shear deformation apparatus is useful for structural geologists, because it can generate very large shear strains that are comparable to geological strains (Jessell & Lister 1991, Passchier & Sokoutis 1993), although such a geometry never occurs in natural deformation. Passchier & Sokoutis (1993) and Passchier *et al.* (1993) utilized a rotational shear apparatus to model the behaviour of porphyroclast systems, whereas Jessell & Lister (1991) analysed strain localization in a rotational shear zone. However, the strain estimate by Passchier & Sokoutis (1993) is not straightforward, and the stress estimate by Jessell & Lister (1991) is ambiguous [in equation (2), p. 433, their r should be the distance from *the centre* of rotation: see later]. The applicability of their experimental results would be more reliable if stress and strain were properly estimated. We present here short comments on stress and strain in a rotational shear zone. We first present stress and strain analyses for Newtonian viscous flow, then expand the analyses into non-Newtonian flow.

SHEAR STRAIN RATE

The stress and strain in a Newtonian material deformed in rotational shear is given by Reiner (1960, pp. 20–34). Figure 1 is a sketch of the boundary conditions of the flow. According to Reiner (1960, p. 22), the parameter that controls the viscous resistance in rotational flow is not the velocity gradient but the shear strain rate ($\dot{\gamma}$). The basic relationship between shear strain rate and tangential shear stress $\tau_{r\theta}$ at a point is $\mu\dot{\gamma} = \tau_{r\theta}$, where μ is the viscosity of the Newtonian material. Shear strain rate at each point in rotational flow is given by

$$\dot{\gamma} = r\frac{\mathrm{d}\dot{\theta}}{\mathrm{d}r}, \tag{1}$$

where r is the distance from the centre of rotation to the point and $\dot{\theta}$ is the angular velocity [equation (22) of Reiner, 1960, p. 22]. The angular velocity for time-independent flow is expressed as a function of r as:

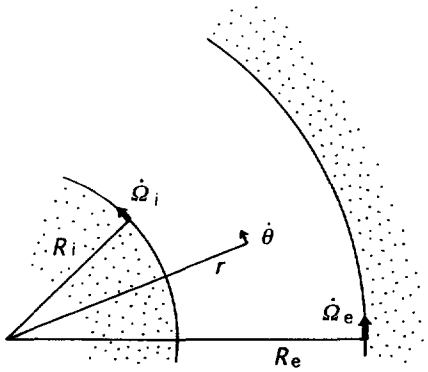

Fig. 1. Sketch of the boundary conditions for rotational shear flow. r and $\dot{\theta}$ are the distance from the centre of rotation and the angular velocity; R_e and R_i, the radii of the external and internal boundaries of the rotational shear zone; and $\dot{\Omega}_e$ and $\dot{\Omega}_i$ the angular velocities at $r = R_e$ and $r = R_i$, respectively.

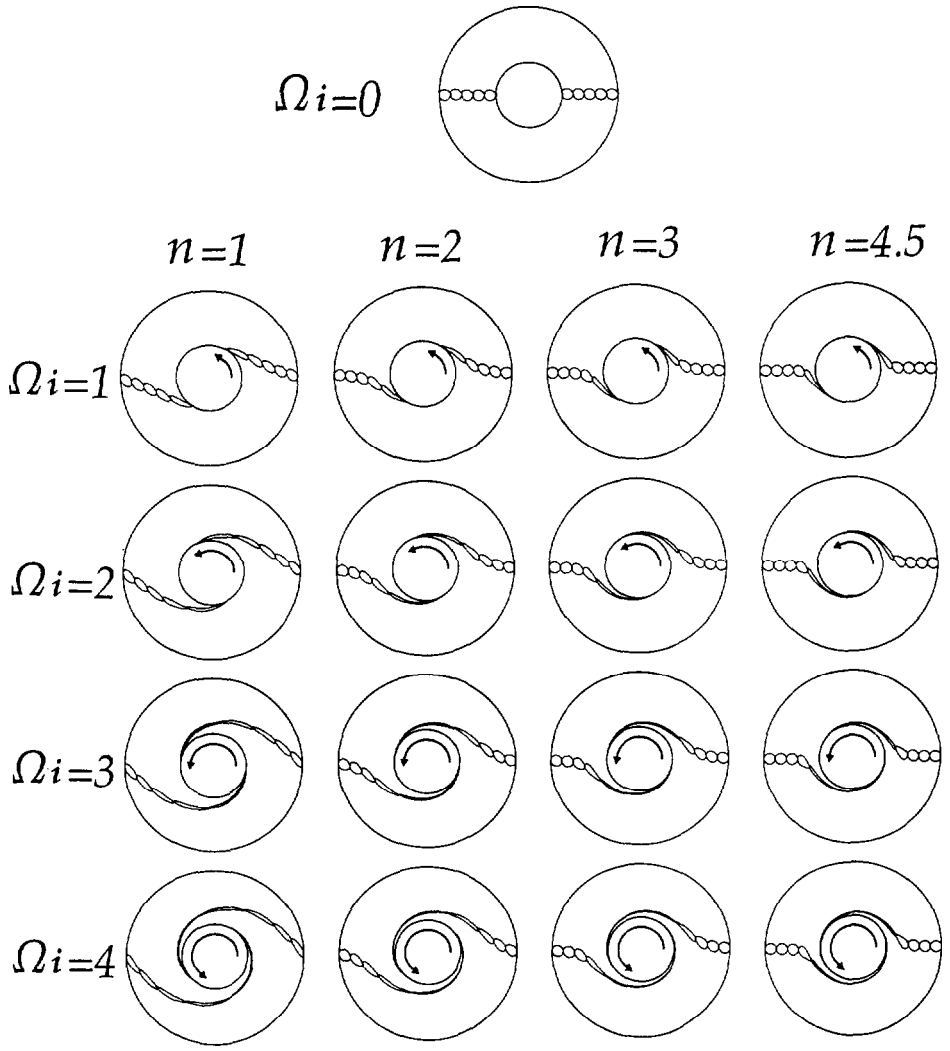

Fig. 2. Deflection of circles during progressive deformation. $\dot{\Omega}_e$ is put as zero in this case. Ω_i indicates the rotation angle of the internal boundary in radians. When $n = 1$. the material is Newtonian. whereas when $n \neq 1$, the material is non-Newtonian.

$$\dot{\theta} = \frac{1}{R_e^2 - R_i^2}\left\{\dot{\Omega}_i R_i^2\left(\frac{R_e^2}{r^2} - 1\right) - \dot{\Omega}_e R_e^2\left(\frac{R_i^2}{r^2} - 1\right)\right\}, \quad (2)$$

where R_e and R_i are the radii of the external and internal boundaries of the rotational shear zone, and Ω_e and Ω_i, the angular velocities at $r = R_e$ and $r = R_i$ respectively [equation (38) of Reiner, 1960, p. 37]. Thus by substituting $\dot{\theta}$ into equation (1), we obtain

$$\dot{\gamma} = \frac{-2(\dot{\Omega}_i - \dot{\Omega}_e)}{\dfrac{1}{R_i^2} - \dfrac{1}{R_e^2}}\frac{1}{r^2}. \quad (3)$$

This equation indicates that shear strain rate is not constant across the shear zone but is proportional to $1/r^2$.

STRAIN ELLIPSES

Figure 2 shows how initial circles of finite radius, set within the rotational shear zone before deformation, change their shapes during progressive deformation. These diagrams are drawn employing the particle-path technique used by Masuda & Ando (1988, p. 343) to show the deflection of marker circles in the simple shear flow. Although the shapes are not ellipses, due to the inhomogeneity of strain rate throughout a rotational shear zone, they provide us with a general idea of the strain intensity as r changes. Inner regions of the shear zone suffer obviously higher strains than outer ones.

STRESS

Stress state in the shear zone is given by the following equations in cylindrical coordinates when the deformation is slow [Lamb 1932, p. 579; equation (11)]:

$$\left.\begin{aligned}\sigma_{rr} &= -p + 2\mu\frac{\partial v_r}{\partial r}\\ \sigma_{\theta\theta} &= -p + 2\mu\left(\frac{1}{r}\frac{\partial v_\theta}{\partial \theta} + \frac{v_r}{r}\right)\\ \tau_{r\theta} &= \mu\left(\frac{1}{r}\frac{\partial v_r}{\partial \theta} - \frac{v_\theta}{r} + \frac{\partial v_\theta}{\partial r}\right)\end{aligned}\right\}, \quad (4)$$

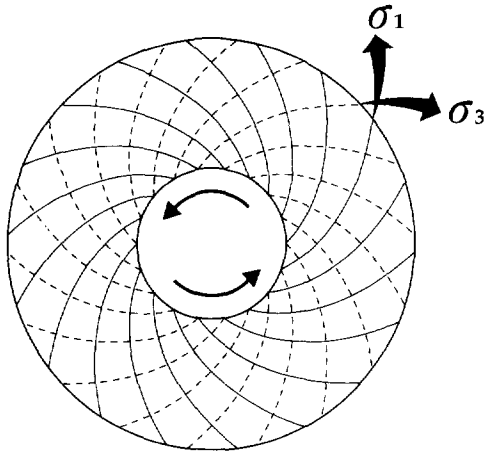

Fig. 3. Stress trajectories in the rotational shear zone. Solid and dashed lines indicate σ_1 and σ_3, respectively.

where v_r and v_θ are velocities parallel to the r and θ axes, respectively, σ_{rr}, $\sigma_{\theta\theta}$ and $\tau_{r\theta}$ are the stress components, and p is the pressure, defined as the mean of σ_{rr} and $\sigma_{\theta\theta}$. As the particles in rotational flow keep a constant distance from the centre (r) during deformation, we put $v_r = 0$, $v_\theta = r\dot{\theta}$ and $\partial v_\theta/\partial \theta = 0$. Substituting these into equation (4), we obtain

$$\left.\begin{aligned} \sigma_{rr} &= -p \\ \sigma_{\theta\theta} &= -p \\ \tau_{r\theta} = \mu\dot{\gamma} &= \frac{\dot{\Omega}_i - \dot{\Omega}_e}{\frac{1}{R_i^2} - \frac{1}{R_e^2}} \frac{-2\mu}{r^2} \end{aligned}\right\}. \tag{5}$$

The trajectories of principal stresses σ_1 and $\sigma_3(\sigma_1 > \sigma_3)$ are calculated from these values (e.g. Jaeger & Cook 1969, pp. 13–14) as shown in Fig. 3. σ_1 and σ_3 at each point are oriented at 45° to the radial axis from the centre of the cylindrical coordinates. The shear stress $\tau_{r\theta}$ is proportional to $1/r^2$.

NON-NEWTONIAN MATERIALS

For a time-independent flow of non-Newtonian materials, the basic equation is given by

$$\dot{\gamma} = k\tau_{r\theta}^n, \tag{6}$$

where $\dot{\gamma}$ $(= r\,\mathrm{d}\dot{\theta}/\mathrm{d}r)$ is the shear strain rate, k is a constant, $\tau_{r\theta}$ is the tangential shear stress and n is the stress exponent [Reiner 1960, p. 244, equation (4)]. Following Reiner's (1960, pp. 244–245) description, we derive the angular velocity $(\dot{\theta})$ as

$$\dot{\theta} = \frac{\dot{\Omega}_i - \dot{\Omega}_e}{\frac{1}{R_i^{2n}} - \frac{1}{R_e^{2n}}} \frac{1}{r^{2n}} + \frac{R_i^{2n}\dot{\Omega}_i - R_e^{2n}\dot{\Omega}_e}{R_i^{2n} - R_e^{2n}}, \tag{7}$$

where R_e, R_i, $\dot{\Omega}_e$ and $\dot{\Omega}_i$ are the same boundary conditions of the shear deformation as those used for the Newtonian material (Fig. 1). Thus, we give $\dot{\gamma}$ as a function of r as

$$\dot{\gamma} = \frac{\dot{\Omega}_i - \dot{\Omega}_e}{\frac{1}{R_i^{2n}} - \frac{1}{R_e^{2n}}} \frac{-2n}{r^{2n}}. \tag{8}$$

Shear strain rate is found to be proportional to $1/r^{2n}$. If we put $n = 1$, then $\dot{\gamma}$ is exactly the same as that of equation (3) for the Newtonian material, and $1/k$ is the viscosity. How initial circles before the deformation are deflected with increasing strain is shown in Fig. 2. Strain gradient close to the internal boundary becomes steeper with increasing n.

The shear stress $r_{r\theta}$ is obtained from equations (6) and (8) as

$$\tau_{r\theta} = \left(\frac{1}{k} \frac{\dot{\Omega}_i - \dot{\Omega}_e}{\frac{1}{R_i^{2n}} - \frac{1}{R_e^{2n}}} \frac{-2n}{r^{2n}} \right)^{1/n}. \tag{9}$$

The shear stress is thus proportional to $1/r^2$ even for the non-Newtonian flow.

In order to know stress trajectories for a non-Newtonian flow, we consider the rheological equations [Tomita, 1975, pp. 257–258; equations (7.17–7.19)]:

$$\begin{aligned} \sigma_{rr} &= -p + 2L\Theta \frac{\partial v_r}{\partial r} \\ \sigma_{\theta\theta} &= -p + 2L\Theta\left(\frac{1}{r}\frac{\partial v_\theta}{\partial \theta} + \frac{v_r}{r}\right) \\ \tau_{r\theta} &= L\Theta\left(\frac{1}{r}\frac{\partial v_r}{\partial \theta} - \frac{v_\theta}{r} + \frac{\partial v_\theta}{\partial r}\right) \\ \Theta &= \left[2\left\{\left(\frac{\partial v_r}{\partial r}\right)^2 + \left(\frac{1}{r}\frac{\partial v_\theta}{\partial \theta} + \frac{v_r}{r}\right)^2\right\}\right. \\ &\quad \left. + \left(\frac{1}{r}\frac{\partial v_r}{\partial \theta} - \frac{v_\theta}{r} + \frac{\partial v_\theta}{\partial r}\right)^2\right]^{[(1/n)-1]/2}, \end{aligned} \tag{10}$$

where L is a constant. For the rotational flow, $v_r = 0$, $v_\theta = r\dot{\theta}$ and $\partial v_\theta/\partial\theta = 0$. Substituting these values into equation (10), gives the following three expressions:

$$\begin{aligned} \sigma_{rr} &= -p, \\ \sigma_{\theta\theta} &= -p, \\ \tau_{r\theta} &= L\dot{\gamma}^{1/n}. \end{aligned} \tag{11}$$

The third of these equations is essentially identical to equation (6), with k in that equation (6) equivalent to $1/L^n$. These values of stresses indicate that trajectories of principal stresses σ_1 and σ_3 for the non-Newtonian flow are the same as those for Newtonian flow (Fig. 3).

REMARKS

(1) Figure 2 shows how n affects the distribution of strain ellipses in the ring shear zone. The deformation

becomes more concentrated in a narrow zone close to the internal boundary as n increases. Jessell & Lister (1991) used OCP (octachloropropane) for their ring shear experiment and showed that strain localization occurred around the internal boundary. Since n for OCP is 4.5 (Bons 1993), the strain localization in OCP is consistent with the distribution of strain ellipses for $n = 4.5$ shown in Fig. 2. However, some results by Jessell & Lister (1991) are not just as predicted for a non-Newtonian viscous material. The differences are presumably due to the deviation of solid-state flow of OCP from power-law viscous flow.

(2) Passchier *et al.* (1993) and Passchier (1994) suggest that n is one of the important parameters that control the shape of porphyroclast systems in mylonites in shear zones. Since the boundary conditions of a ring shear deformation are different from those of natural shear zones, the shapes of the strain ellipses shown in Fig. 2 are hardly equivalent to those around porphyroclasts in mylonites. However, the general tendency for localization of deformation with different n demonstrated in Fig. 2 may be an important clue for inferring the magnitude of n of the natural matrix around porphyroclasts.

Acknowledgements—We thank H. Nagahama for the comments on the equations, A. Nakayama for constructive discussions on non-Newtonian flow, P. J. Hudleston for encouraging comments on the manuscript, and one anonymous reviewer for correcting English.

REFERENCES

Bons, P. D. 1993. Experimental deformation of polyphase rock analogues. *Geologica Ultrajectina* 110, Mededelingen van de Faculteit Aardwetenschappen der Universiteit Utrecht.

Jaeger, J. C. & Cook, N. G. W. 1969. *Fundamentals of Rock Mechanics*. Methuen, London.

Jessell, M. W. & Lister, G. S. 1991. Strain localization behaviour in experimental shear zones. *Pure & Appl. Geophys.* **137**, 421–438.

Lamb, H. 1932. *Hydrodynamics*. Cambridge University Press, New York.

Masuda, T. & Ando, S. 1988. Viscous flow around a rigid spherical body; a hydrodynamical approach. *Tectonophysics* **148**, 337–346.

Passchier, C. W. 1994. Mixing in flow perturbations: a model for development of mantled porphyroclasts. *J. Struct. Geol.* **16**, 733–736.

Passchier, C. W. & Sokoutis, D. 1993. Experimental modelling of mantled porphyroclasts. *J. Struct. Geol.* **15**, 895–909.

Passchier, C. W., Ten Brink, C. E., Bons, P. D. & Sokoutis, D. 1993. δ objects as a gauge for stress sensitivity of strain rate in mylonites. *Earth Planet. Sci. Lett.* **120**, 239–245.

Reiner, M. 1960, *Deformation, Strain, and Flow: An Elementary Introduction to Rheology*. Lewis & Co. Ltd, London.

Tomita, Y. 1975. *Rheology*. Corona Publishing, Tokyo. (A textbook on Rheology written in Japanese.)